

# Search for Charged Higgs Bosons in $e^+e^-$ Collisions at DELPHI

Mattias Ellert<sup>a</sup>, Marco Battaglia<sup>b</sup>, Tord Ekelöf<sup>a</sup>, Guillelmo Gómez-Ceballos<sup>c</sup>, Ari Kiiskinen<sup>b</sup>, Pierre Lutz<sup>d</sup>, Francisco Matorras<sup>c</sup>

<sup>a</sup>Uppsala University, Department of Radiation Sciences, Box 535, SE-751 21 Uppsala, Sweden

<sup>b</sup>Helsinki Institute of Physics, P.O. Box 9, FI-00014 Helsinki, Finland

<sup>c</sup>Instituto de Física de Cantabria, Avda. los Castros s/n, ES-39006 Santander, Spain

<sup>d</sup>DAPNIA/Service de Physique des Particules, CEA-Saclay, FR-91191 Gif-sur-Yvette Cedex, France

A search for pair produced charged Higgs bosons was performed using the data collected by the DELPHI detector at LEP II at centre-of-mass energies up to 208 GeV. The three different final states,  $\tau\nu\tau\nu$ ,  $c\bar{s}\tau\nu$  and  $c\bar{s}c\bar{s}$  were considered. No excess of data compared to the expected Standard Model processes was observed and the existence of a charged Higgs boson with mass lower than 75.0 GeV/ $c^2$  has been excluded at 95% confidence level.

## 1. Introduction

The existence of a charged Higgs boson is predicted by several extensions of the Standard Model. Pair production of charged Higgs bosons occurs mainly via  $s$ -exchange of a photon or a  $Z^0$  boson. In two-doublet models, the couplings are completely specified in terms of the electric charge and the Weinberg angle,  $\theta_W$ , and therefore the production cross-section depends only on the charged Higgs boson mass. Higgs bosons decay predominantly to the heaviest fermions kinematically allowed, which in the case of charged Higgs bosons at LEP energies can be either a  $\tau\nu_\tau$  pair or a  $cs$  quark pair. In order to ensure that the results are model independent the decay branching fraction has been treated as a free parameter in the analysis. The search was based on the first 74 pb<sup>-1</sup> of data collected by DELPHI in the year 2000 at centre-of-mass energies up to 208 GeV. The results have been combined with those obtained in an analysis of earlier DELPHI data [1].

## 2. Data Analysis

The DELPHI detector and its performance have been described in detail elsewhere [2,3].

Signal samples were simulated using PYTHIA [4]. The background estimates from different

Standard Model processes were based on the following event generators: PYTHIA for  $q\bar{q}(\gamma)$ , KORALZ [5] for  $\mu^+\mu^-$  and  $\tau^+\tau^-$ , BAFO [6] for  $e^+e^-$  and EXCALIBUR [7] for four-fermion final states. Two-photon interactions were generated with TWOGAM [8] for hadronic final states, BDK and BDKRC [9] for leptonic final states.

In all three channels the final background rejection was performed by using a likelihood technique. For each of the  $N$  discriminating variables, the fractions  $F_i^{\text{HH}}(x_i)$  and  $F_i^{\text{bkg}}(x_i)$  of respectively  $H^+H^-$  and background events corresponding to a given value  $x_i$  of the  $i^{\text{th}}$  variable, were extracted from a sample of simulated background and  $H^+H^-$  events with equal populations. The signal likelihood was computed as the normalised product of these individual fractions,  $\prod_{i=1}^N F_i^{\text{HH}}(x_i) / (\prod_{i=1}^N F_i^{\text{HH}}(x_i) + \prod_{i=1}^N F_i^{\text{bkg}}(x_i))$ .

### 2.1. The leptonic channel

Events in this channel have large missing energy and momentum and two acollinear and acoplanar jets containing either a lepton or one or a few hadrons. Tighter requirements were used in this channel on good running of the most important sub-detectors in order to ensure good quality of the tracks.

### 2.1.1. Event preselection

To select leptonic events a total charged particle multiplicity between 2 and 6 was required. All particles in the event were clustered into jets using the LUCLUS algorithm [4] ( $d_{join} = 6.5 \text{ GeV}/c^2$ ) and only events with two reconstructed jets both containing at least one charged particle and at least one jet with only one charged particle were retained. Events with an invariant mass of either of the jets of more than  $3 \text{ GeV}/c^2$  were rejected.

The cosine of the polar angle of the leading track of each jet, i.e. the particle with the highest momentum, was required to be less than 0.98. The event acoplanarity was required to be less than  $13^\circ$  ( $25^\circ$ ) if both leading tracks were (were not) in the barrel region, the total energy component transverse to the beam direction was required to be greater than  $0.08\sqrt{s}$  ( $0.1\sqrt{s}$ ) and the total transverse momentum to be greater than  $0.04\sqrt{s}$ . Also events with a total energy detected within  $30^\circ$  around the beam axis of more than  $0.1\sqrt{s}$  or an acollinearity of more than  $150^\circ$  were rejected.

If a particle from a  $\tau$  decay was identified as an electron it had to have a momentum below  $0.13\sqrt{s}$  and an electromagnetic energy below  $0.14\sqrt{s}$ . If identified as a muon, the momentum had to be below  $0.13\sqrt{s}$ . If the  $\tau$  decay particle was neither identified as a muon nor an electron, it was considered a hadron.

### 2.1.2. Final background rejection

After these selections most of the remaining background is  $W^+W^- \rightarrow \tau^+\nu_\tau\tau^-\bar{\nu}_\tau$  events. Events from both the  $H^+H^-$  signal and the  $W^+W^-$  background have similar topologies and due to the presence of missing neutrinos in the decay of each of the bosons it is not possible to reconstruct the boson mass. Two important differences, however, were used in order to discriminate the signal and the  $W^+W^-$  background: the boson polar angle and the  $\tau$  polarisation.

Assuming that the  $\nu_\tau$  has a definite helicity, the polarisation of  $\tau$ 's originating from heavy boson decays is determined entirely by the properties of weak interactions and the nature of the parent boson. The helicity configuration for the signal

is  $H^- \rightarrow \tau_R^- \bar{\nu}_{\tau R}$  ( $H^+ \rightarrow \tau_L^+ \nu_{\tau L}$ ) and for the  $W^\pm$  boson background it is  $\bar{W}^- \rightarrow \tau_L^- \bar{\nu}_{\tau R}$  ( $W^+ \rightarrow \tau_R^+ \nu_{\tau L}$ ) resulting in  $P_\tau^H = +1$  and  $\bar{P}_\tau^W = -1$ . The angular and momentum distributions depend on polarisation and it is possible to build estimators of the  $\tau$  polarisation to discriminate between the two contributions.

The  $\tau$  decays were classified into the following categories: electron, muon,  $\pi$ ,  $\pi + n\gamma$ ,  $3\pi$  and others. The information on the  $\tau$  polarisation was extracted from the observed kinematic distributions of its decay products, e.g. angles and momenta [10]. For charged Higgs boson masses close to the threshold, the boost of the bosons is relatively small and the  $\tau$  energies are similar to the  $\tau$ 's from  $Z^0$  decays (40–50 GeV).

A likelihood to separate the signal from the background was built using four variables: the estimators of the  $\tau$  polarisation and the boson polar angle of both  $\tau$ 's. The distribution of the likelihood for data, expected backgrounds and signal is shown in Figure 1.

The number of selected events after the different cuts are shown in Table 1.

Table 1: Number of selected events and signal efficiency in the leptonic channel.

cut	data	bkg.	eff.
2-jet selection	221	211.0	55.0%
angular cuts	80	85.4	47.3%
$\tau$ ID	15	10.0	35.6%
final selection	12	8.8	33.2%

## 2.2. The hadronic channel

In the fully hadronic decay channel, each charged Higgs boson is expected to decay into a  $c\bar{s}$  pair, producing a four-jet final state. The two sources of background in this channel are the  $q\bar{q}g$  QCD background and fully hadronic four-fermion final states.

### 2.2.1. Event preselection

The first level hadronic four-jet event selection used in this analysis is the same as in the DELPHI neutral Higgs analysis [11].

Events were clustered into four jets using the Durham algorithm [12] and the  $y_{4 \rightarrow 3}$  ( $y_{5 \rightarrow 4}$ ) clustering distance was required to be greater than 0.003 (less than 0.010).

Energy and momentum conservation was imposed by performing a 4C fit. A 5C fit, assuming equal boson masses, was applied in order to improve the resolution on the di-jet mass. Of the three possible jet pairings the one giving the smallest  $\chi^2$  was selected. Events for which the  $\chi^2$  per degree of freedom for this pairing exceeded 1.5 or for which the difference between the di-jet masses computed after the 4C fit exceeded  $10 \text{ GeV}/c^2$  were rejected.

### 2.2.2. Final background rejection

The largest contribution to the part of the selected sample having reconstructed masses below  $75 \text{ GeV}/c^2$  is  $W^+W^-$  events with wrong di-jet pairing. These wrongly paired events are characterised by larger difference between the masses of the two di-jets.

Since the initial quarks of a quark-antiquark pair resulting from a boson decay are connected by a QCD colour string, in which the hadrons are produced in the fragmentation process, wrongly paired quark pairs can be identified using a method of colour connection reconstruction [13]. This method is based on the fact that in the rest frame of the correctly paired initial quark-antiquark pair the hadrons that are produced in the colour string should have vanishing transverse momenta relative to the quark-antiquark pair axis. When boosted into a rest frame of a wrongly paired quark pair the transverse momenta of the particles relative to the quark-quark axis are larger. The correct pairing is found by calculating the sum of transverse particle momenta in each of the three possible pairing hypotheses. The pairing chosen using the colour connection reconstruction is compared to the pairing chosen using the minimisation of  $\chi^2$  of the kinematical fit. The outcome of this comparison, the  $p_\perp$ -veto, is binary information: agreement or disagreement.

The production polar angle of the positively charged boson is reconstructed as the polar angle of the di-jet with higher charge where the jet charge is calculated as a momentum weighted sum of the charges of the tracks in the jet.

The charged Higgs boson is expected to couple predominantly to  $c\bar{s}$  in its hadronic decay mode. A flavour tagging algorithm has been developed

for the study of multiparton final states [14]. This tagging is based on nine discriminating variables: three of them are related to the identified lepton and hadron content of the jet, two depend on kinematical variables and four on the reconstructed secondary decay structure. The finite  $c$  lifetime is exploited to distinguish between  $c$  and light quark jets, while the  $c$  mass and decay multiplicity, is used to discriminate against  $b$  jets. Furthermore  $s$  and  $c$  jets can be distinguished from  $u$  and  $d$  jets by the presence of an identified energetic kaon. The responses for the individual jets are further combined into an event  $c\bar{s}c\bar{s}$  probability.

The four variables described above: the di-jet pair mass difference, the  $p_\perp$ -veto, the di-jet momentum polar angle and the event  $c\bar{s}c\bar{s}$  probability were combined to form an event anti-WW likelihood function separating  $W^+W^-$  events from  $H^+H^-$  events.

QCD background events differ also kinematically from pair-produced bosons [15]. In order to reject the QCD background more effectively the following variables were used in the anti-QCD likelihood in addition to the four above: the  $y_{4\rightarrow 3}$  clustering distance and the event acoplanarity.

The reconstructed mass distribution for data, simulated backgrounds and signal after anti-QCD and anti-WW cuts is shown in Figure 1.

The number of selected events after the different cuts are shown in Table 2.

Table 2: Number of selected events and signal efficiency in the hadronic channel.

cut	data	bkg.	eff.
4-jet selection	677	649.0	78%
$\chi^2$	496	482.4	62%
likelihoods	147	127.2	33%

### 2.3. The semileptonic channel

In this channel one of the charged Higgs bosons decays into a  $c\bar{s}$  quark pair, while the other decays into  $\tau\nu_\tau$ . Such an event is characterised by two hadronic jets, a  $\tau$  candidate and missing energy carried by the neutrinos. The dominating background processes are QCD  $q\bar{q}g$  events and semileptonic decays of  $W^+W^-$ .

### 2.3.1. Event preselection

At least 15 particles, of which at least 8 charged particles, were required to be reconstructed in the event to be considered for analysis. The total energy of the observed particles had to exceed  $0.30\sqrt{s}$ . The missing transverse momentum had to be greater than  $0.08\sqrt{s}$  and the cosine of the angle between the missing momentum and the beam pipe had to be greater than 0.8. Events were also required to have no neutral particles with energy above 40 GeV.

After clustering into three jets using the Durham algorithm, the clustering distance  $y_{3\rightarrow 2}$  was required to be greater than 0.003, and each jet had to contain at least one charged particle. The jet with the smallest charged particle multiplicity was treated as the  $\tau$  candidate and if more than one of the jets had the same number of charged particles, the one with smallest energy was chosen. The  $\tau$  candidate was required to have no more than six particles, of which no more than three charged.

### 2.3.2. Final background selection

The mass of the decaying bosons was reconstructed using a fit requiring energy and momentum conservation and equal boson masses. The three components of the momentum vector of the  $\nu_\tau$  and the magnitude of the  $\tau$  momentum were treated as free parameters, reducing the number of degrees of freedom of the fit from 5 to 1. Only events with a reconstructed mass above 40 GeV/ $c^2$  and a  $\chi^2$  below 2 were selected.

To define the anti-QCD likelihood the acollinearity of the event, the polar angle of the missing momentum, the logarithm of the clustering distance  $y_{3\rightarrow 2}$  and the product of the  $\tau$  jet energy and the smallest of the angles between the  $\tau$  jet and one of the other jets were used as discriminating variables.

For the event anti-WW likelihood the variables used were the reconstructed polar angle of the negatively charged boson (where the charge was taken to be that of the leading charged particle of the  $\tau$  jet), the angle between the boson and the  $\tau$  in the boson rest frame, the energy of the  $\tau$  jet, the classification of the decay of the  $\tau$  candidate ( $e, \mu, \pi, \pi + n\gamma, 3\pi$  and others), and the

$cs$  probability of the hadronic di-jet.

The reconstructed mass distribution for data, simulated backgrounds and signal after anti-QCD and anti-WW cuts is shown in Figure 1.

The number of selected events after the different cuts are shown in Table 3.

Table 3: Number of selected events and signal efficiency in the semileptonic channel.

cut	data	bkg.	eff.
preselection	1273	1139	82.2%
$\tau$ selection	414	418	60.0%
$\chi^2$	330	342	50.9%
likelihoods	59	72.5	38.5%

## 3. Results

No excess of events compared to the expected backgrounds was observed in any of the three different final states investigated. A lower limit for a charged Higgs boson mass was derived at 95% confidence level as a function of the leptonic Higgs decay branching ratio  $\text{BR}(H \rightarrow \tau\nu_\tau)$ . The confidence in the signal hypothesis,  $CL_s$ , was calculated using a likelihood ratio technique [16].

The background and signal probability density functions of one or two discriminating variables in each channel were used. In the hadronic and semileptonic channels the two discriminating variables were the reconstructed mass and the anti-WW likelihood while in the leptonic channel only one background discrimination likelihood was used because mass reconstruction is not possible. The distributions for the discriminating variable of signal events, obtained by the simulation at different  $H^\pm$  mass values for each  $\sqrt{s}$ , were interpolated for intermediate mass values. The signal efficiencies were fitted with polynomial functions, to obtain the expected signal rate at any given mass.

The results are summarised in Figure 2. Independently of the hadronic decay branching ratio a lower  $H^\pm$  mass limit of  $M_{H^\pm} > 75.0$  GeV/ $c^2$  can be set at 95% confidence level.

## 4. Conclusion

A search for charged Higgs bosons was performed using data collected by DELPHI at

## DELPHI preliminary

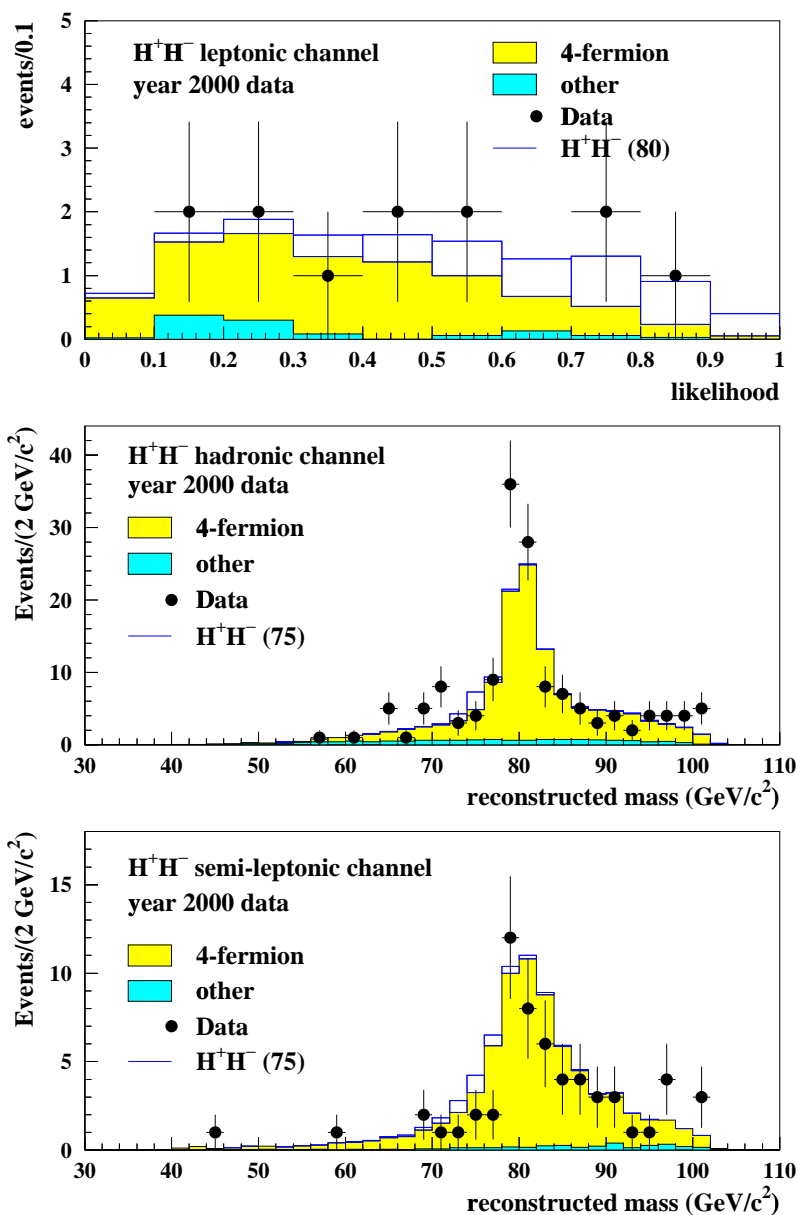


Figure 1. The distribution of the background rejection likelihood for the leptonic channel and the distribution of reconstructed mass for the hadronic and the semileptonic channels. All plots have been produced using data collected during the year 2000 runs corresponding to an integrated luminosity of 74 pb<sup>-1</sup>.

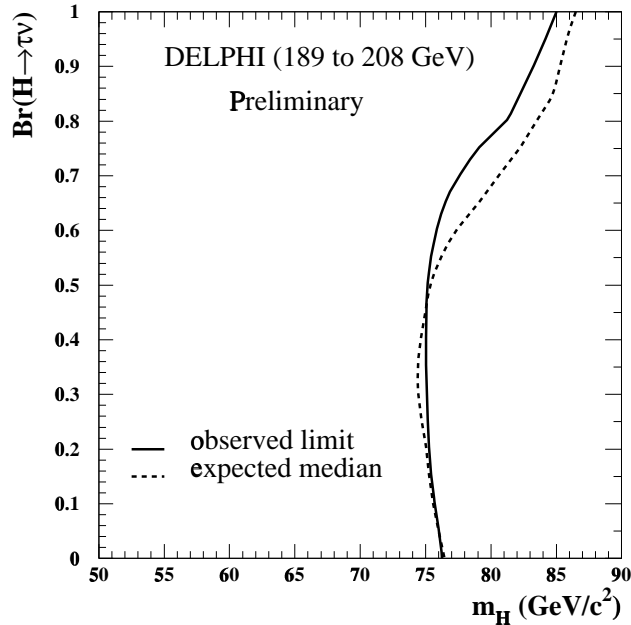


Figure 2. The 95% CL mass exclusion limit as a function of the leptonic branching ratio using combination of DELPHI data from 189 GeV up to 208 GeV.

centre-of-mass energies up to 208 GeV analysing the  $\tau\nu\tau\nu$ ,  $c\bar{s}\tau\nu$  and  $c\bar{s}c\bar{s}$  final states. No significant excess of candidates was observed and a lower limit on the charged Higgs boson mass of  $75.0 \text{ GeV}/c^2$  was set at 95% confidence level.

#### Acknowledgements

We are greatly indebted to our technical collaborators, to the members of the CERN-SL Division for the excellent performance of the LEP collider, and to the funding agencies for their support in building and operating the DELPHI detector.

#### REFERENCES

1. M. Battaglia *et al.*, DELPHI 2000-091 CONF 390, contributed paper no 613 to ICHEP 2000
2. P. Aarnio *et al.*, Nucl. Instr. and Meth. **A 303** (1991) 223
3. P. Abreu *et al.*, Nucl. Instr. and Meth. **A 378** (1996) 57
4. T. Sjöstrand, Comp. Phys. Comm. **82** (1994) 74
5. S. Jadach, B. F. L. Ward and Z. Was, Comp. Phys. Comm. **79** (1994) 503
6. F. A. Berends, R. Kleiss and W. Hollik, Nucl. Phys. **B 304** (1988) 712
7. F. A. Berends, R. Pittau and R. Kleiss, Comp. Phys. Comm. **85** (1995) 437
8. S. Nova, A. Olcheski and T. Todorov, in CERN Report 96-01, Vol. 2. p.224
9. F. A. Berends, P. H. Daverveldt and R. Kleiss, Comp. Phys. Comm. **40** (1986) 271, 285, 309
10. P. Abreu *et al.*, Zeit. Phys. **C 67** (1995) 183
11. P. Abreu *et al.*, E. Phys. J. **C 10** (1999) 563
12. S. Catani *et al.*, Phys. Lett. **B 269** (1991) 432
13. A. Kiiskinen *et al.*, DELPHI 98-91 CONF 159, contributed paper no 151 to ICHEP 1998
14. P. Abreu *et al.*, Phys. Lett. **B 439** (1998) 209
15. P. Abreu *et al.*, E. Phys. J. **C 2** (1998) 581
16. A. L. Read, DELPHI 97-158 PHYS 737, public DELPHI note